ACS APPLIED MATERIALS & INTERFACES

www.acsami.org

Research Article

Insights into Mechanical Dynamics of Nanoscale Interfaces in Epoxy Composites Using Nanorheology Atomic Force Microscopy

Hung K. Nguyen, Atsuomi Shundo, Makiko Ito, Bede Pittenger, Satoru Yamamoto, Keiji Tanaka,* and Ken Nakajima*

Cite This: *ACS Appl. Mater. Interfaces* 2023, 15, 38029−38038

Read Online

ACCESS | Metrics & More | Article Recommendations | Supporting Information

ABSTRACT: Interfacial polymer layers with nanoscale size play critical roles in dissipating the strain energy around cracks and defects in structural nanocomposites, thereby enhancing the material's fracture toughness. However, understanding how the intrinsic mechanical dynamics of the interfacial layer determine the toughening and reinforcement mechanisms in various polymer nanocomposites remains a major challenge. Here, by means of a recently developed nanorheology atomic force microscopy method, also known as nanoscale dynamic mechanical analysis (nDMA), we report direct mapping of dynamic mechanical responses at the interface of a model epoxy nanocomposite under the transition from a glassy to a rubbery state. We demonstrate a significant deviation in the dynamic moduli of the interface from matrix behavior. Interestingly, the sign of the deviation is observed to be reversed when the polymer changes from a glassy to a rubbery state, which provides an excellent explanation for the difference in the modulus reinforcement between glassy and rubbery epoxy nanocomposites. More importantly, nDMA loss tangent images unambiguously show an enhanced viscoelastic response at the interface compared to the bulk matrix in the glassy state. This observation can therefore provide important insights into the nanoscale toughening mechanism that occurs in epoxy nanocomposites due to viscoelastic energy dissipation at the interface.

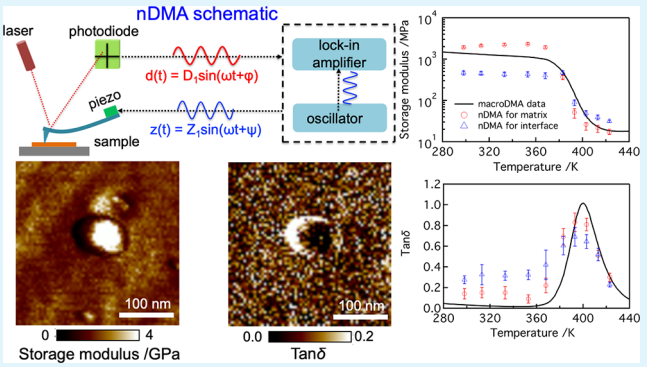

KEYWORDS: *nDMA−AFM, nanoscale interface, mechanical dynamics, viscoelasticity, fracture toughness, epoxy nanocomposite*

1. INTRODUCTION

Over the past two decades, numerous polymer-based composites have been developed for use as lightweight materials in the automotive, aerospace, and civil engineering industries.[1−4] Among polymer materials, epoxy resins offer attractive opportunities for such applications because they can be used not only as a matrix in structural composites, such as fiber-reinforced epoxies, but also as adhesive bonding components for replacing conventional mechanical joining techniques, thanks to their excellent adhesion, high mechanical strength, thermal stability, and chemical resistance.[5−9] The primary limitation of epoxy resins is their poor resistance to crack initiation and propagation. Recent efforts to incorporate micro/nanofillers into epoxy matrices have had great success in overcoming this limitation.[9−13] Using soft polymers as a dispersed phase in epoxy resins has been a common way to improve the epoxy's toughness. In this combination, the toughening mechanism can be attributed to the viscoelastic behavior of the soft polymer phase to dissipate local strain energy near cracks.[14−16] Unexpectedly, a similar achievement for the improvement of epoxy toughness was also reported in many studies when using rigid fillers such as nanosilica.[17−21] The advantage of using rigid fillers over soft ones is that they can enhance the fracture toughness without sacrificing various intrinsic thermomechanical properties of epoxies.[17−19] Consequently, many types of rigid nanoparticles, such as silica, alumina, graphite, graphene, and carbon nanotubes, have been extensively investigated for toughening epoxy resins.[22−27] However, the physical mechanism underlying this toughening effect has not been fully understood so far.[9,13,28,29]

Attempts in many theoretical and experimental studies have provided growing evidence that the toughening effect in epoxy nanocomposites is largely governed by the nanoscale interfaces that are formed between nanoparticles and epoxy matrices.[13,29−33] In particular, the alteration in both structural and physical properties of polymers at the interface from matrix behavior is thought to play critical roles in dissipating the strain energy via several types of nanoscopic events, such as the debonding of nanoparticles, local plastic deformation, and

Received: April 28, 2023
Accepted: July 17, 2023
Published: July 27, 2023

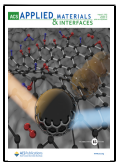

nanovoid generation.[13,29,34,35] This scenario is indeed strongly supported by recent experimental results based on various characterization techniques at the nanoscale.[36−38] For example, Sirovica and co-workers have evidenced a reduction of the crosslinking density in an epoxy network near the silica particle interface by using synchrotron-based wide field infrared imaging combined with atomic force microscopy (AFM)−infrared spectroscopy.[37] More recently, we have proven the existence of an interfacial epoxy layer with a thickness of ∼20 nm surrounding nanosilica using a bimodal amplitude- and frequency-modulated (AM−FM) AFM.[38] The AM−FM images also revealed a decrease in both elastic and adhesive responses at this interface compared to the matrix region, thus providing a consistent explanation of the preferential debonding process and subsequent generation of nanovoids at the epoxy/silica interface.[19,21,29]

Nevertheless, the changes in such quasi-static properties, i.e., elastic modulus and crosslinking density, of the interfacial layer might not provide a relevant interpretation for other toughening mechanisms that have been seen in various structured nanocomposites and are not directly correlated to the debonding process.[28,39−41] In fact, several energy dissipation processes related to the dynamic relaxation properties of nanoscale interfaces, such as viscosity, friction, and/or viscoelasticity, have been suggested for understanding toughening mechanisms in various hard nanostructured biomaterials containing soft polymer interfaces.[42,43] In a recent report, by means of in situ transmission electron microscopy (TEM) combined with digital image correlation analysis of the strain field for epoxy nanocomposite films under tensile deformation, Wang and co-workers have enabled visualizing the debonding process together with the distribution of the tensile strain in front of the crack tip.[41] They observed the generation and growth of nanovoids surrounding nanoparticles, which were located very close to the crack tip (within ∼1 μm), accompanied by a drastically reduced local strain at these interfaces, as expected. Interestingly, such a local strain constraint was also found surrounding large nanoparticles located quite far from the crack tip by a distance of a few micrometers, where the nanovoids were not observed.[41] This finding shows clear evidence that some dynamic properties occurring at the epoxy/silica interface that are different from plastic relaxation events can contribute to the dissipation of strain energy. For the case of epoxy nanocomposites having a high interfacial volume fraction, such as epoxy films filled with dense packing of multiwalled carbon nanotube (MCNT) fillers,[28] enhanced viscoelasticity at the interface has been suggested relying on macroscopic measurements with a standard rheology technique. However, for epoxies filled with more common rigid nanofillers, such as silica and alumina, it remains difficult to quantify interfacial dynamic properties when using a macroscopic rheological technique.[44,45] Therefore, characterization methods able to address the local rheological properties of the nanoscale interfaces are strongly demanded for better understanding the fundamental mechanisms underlying the toughening and reinforcement effects in epoxy nanocomposites.

Over the past few years, various AFM-based dynamic modes have been developed for quantitative measurements of mechanical dynamics of soft materials at nanoscale,[46−56] among which the nanorheological approaches, also called nanoscale dynamic mechanical analysis (nDMA), have been proven capable of detecting local polymer viscoelasticity in nanostructured systems at rheologically relevant frequencies, that is, from ∼0.1 to ∼100 Hz.[52−56] However, because a sample-driving system is commonly used for performing rheological measurements in most of these approaches, it is only suitable for viscoelastic measurements of soft materials at room temperature. To circumvent this problem, a new design in which a piezo based probe-driving system is placed near the base of an AFM probe has been recently developed,[57−59] enabling the use of a heater/cooler stage beneath the sample for controlling the sample temperature. Indeed, this new approach has been demonstrated to be capable of measuring the mechanical relaxation properties of polymers in both glassy and rubbery states over a broad temperature range.[58]

In this study, we employ this new nDMA approach for directly mapping mechanical relaxation dynamics at the epoxy/silica interface in a model amine-cured epoxy resin nanocomposite. For this system in the glassy state, several methods, including AM−FM AFM and TEM,[38,41] as discussed above, have been employed to detail the effects of the interface on the elastic properties and fracture behavior of the nanocomposite. By using nDMA here, we are able to directly prove the enhancement of the viscoelasticity at the nanoscale interfacial layer compared to the glassy matrix. In addition, nDMA storage modulus maps reveal, for the first time in real space, a change of the interface elasticity from softening to stiffening in comparison with the matrix behavior under the transition from a glassy to a rubbery state.

2. EXPERIMENTAL SECTION

2.1. Materials and Sample Preparation. The neat amine-cured epoxy resin used here was formed based on hydrogenated bisphenol A diglycidyl ether (HDGEBA) and 1,4-cyclohexanebis(methylamine) (CBMA), and its nanocomposite was filled with nanosilica of different weight fractions from 5 to 15 wt %.[38] HDGEBA and CBMA were supplied by New Japan Chemical Co., Ltd., Japan, and Tokyo Chemical Industry Co., Ltd., Japan, respectively. Silica nanoparticles with a mean diameter of 50 nm and a surface modified by phenyl-type silane were purchased from Admatechs Co., Ltd., Japan. All materials were used as received. Details on the sample preparation and thermomechanical properties of the resulting samples have been reported elsewhere.[38,60] Briefly, for the nanocomposite sample, silica nanoparticles were first thoroughly dispersed in CBMA, which was then mixed with HDGEBA at a molar ratio of 1:2, that is, equivalent to the stoichiometry of the epoxy and amino groups. The mixtures were cured at 373 K for 24 h to obtain epoxy-amine systems with a network conversion of nearly 100%. The glass transition temperatures (T_g) for the neat epoxy and epoxy nanocomposites samples were 365 ± 1 K, measured by differential scanning calorimetry (Discovery DSC2500, TA Instruments).[38] For AFM measurements, epoxy nanocomposite films with a thickness of ∼1 μm were prepared by microtome sectioning with an ultramicrotome (UC6, Leica Microsystems, Germany) at 193 K and mounted on clean silicon substrates. Prior to AFM measurements, the system was heated to 423 K for 30 min to remove the thermal history and increase the adhesion between the epoxy nanocomposite films and silicon substrate, followed by a cooling with a speed of 10 K/min to room temperature. Such a heating procedure was confirmed not to affect the mechanical responses of polymers in the matrix and at the interface.

2.2. Dynamic Mechanical Analysis. Macroscopic mechanical relaxation properties of the neat HDGEBA/CBMA and nanocomposites were characterized using the macroscopic dynamic mechanical analysis (macroDMA) technique (Rheovibron DDV-01FP, A&D Co., Ltd., Japan). The fully cured sample was cut into trip specimens with a thickness of 300 μm, a width of 3 mm, and a length of 30 mm. The measurements were performed under a dry nitrogen purge from 273 to 443 K at a heating rate of 2 K/min. A sinusoidal

https://doi.org/10.1021/acsami.3c06123
ACS Appl. Mater. Interfaces 2023, 15, 38029−38038

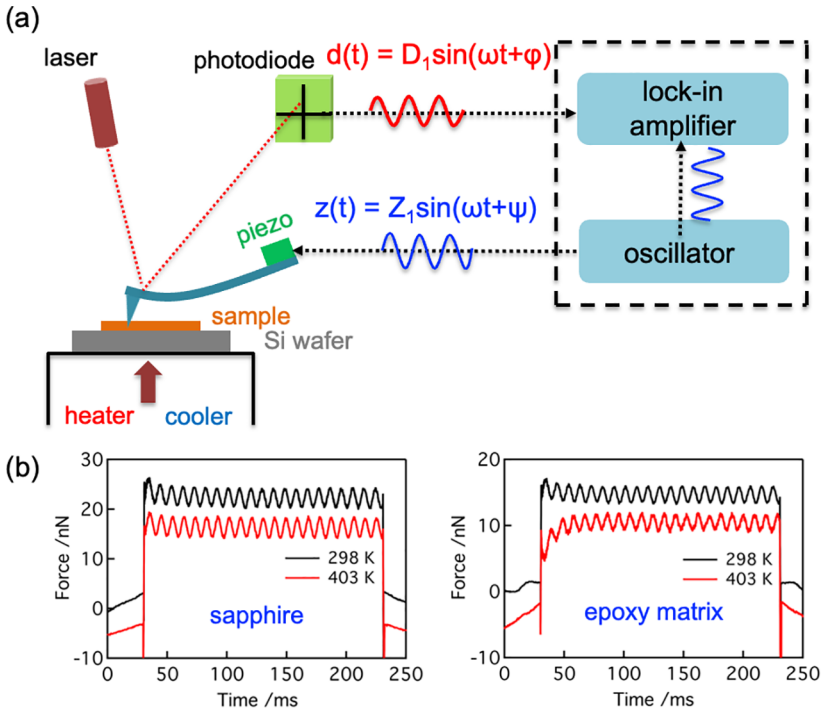

Figure 1. (a) Schematic diagram of nDMA with the probe-driving system. (b) Representative examples of several force modulation versus time plots with nDMA measurements at 105 Hz on the sapphire and epoxy matrix at 298 and 403 K. The data are vertically shifted for clarity.

strain of 0.03%, which was within the linear response regime, was imposed on the specimen at oscillation frequencies ranging from 1 to 110 Hz.

2.3. PeakForce Quantitative Nanomechanical Mapping. Quantitative nanomechanical mapping (QNM) measurements were carried out using NanoScope V together with a MultiMode 8 (Bruker, USA) at a frequency of 1.0 kHz. QNM modulus maps were measured at a resolution of 256 × 256 pixels at room temperature (~298 K) using AC200TS probes (Olympus, Tokyo, Japan). The spring constant and tip radius values of the probe were calibrated to be ~10 N/m and ~8 nm, respectively. The elastic modulus map in the QNM method was obtained by fitting the recorded force-deformation curves using the Johnson−Kendal−Roberts (JKR)-based linearized method.[61,62]

2.4. Nanoscale Dynamic Mechanical Analysis. The nDMA measurements were performed in a Bruker Dimension Icon AFM with a Nanoscope 6 controller (Bruker, USA). nDMA maps were measured at a resolution of 64 × 64 pixels at different temperatures ranging from 298 to 423 K using standard force modulation AFM probes with an aluminum reflective coating (Multi75Al-G, Budget-sensors). The sample temperature was controlled using a Lakeshore model 335 temperature controller. The spring constant and tip radius values of the probe were calibrated to be ~3.3 N/m and ~11 nm, respectively.

Figure 1a shows a schematic diagram of the nDMA method. In this study, we focus on the imaging purpose, for which the measurements are embedded into the force curve-based mapping mode. This approach has been previously described by Pittenger and co-workers,[58] and here, only a brief description is provided. At each pixel point, the probe was first moved toward the sample at a ramp size of about 300 nm and a ramp rate of 10 Hz. When the probe deflection reached a repulsive (trigger) force of 10−20 nN, a sinusoidal signal at a frequency of 105 Hz was applied to the piezo over a period of ~200 ms. The unloading curve at a ramp rate of 10 Hz was then used to calculate the contact radius between the probe and the sample using the JKR-based linearized method (Figure S1). In principle, the applied frequency can vary from 0.1 to 300 Hz. However, the measurement at too low frequencies precludes high imaging speed.[58] Here, a frequency of 105 Hz was used to make imaging moderately high but still comparable to relevant frequencies of the conventional macroDMA technique. At this condition, it took about 20 min to obtain a 64 × 64 pixel image. Details about the theoretical description of the piezo and probe oscillations as well as the calculation of dynamic mechanical quantities including storage modulus, loss modulus, and tan δ of polymers are provided in the Supporting Information. Figure 3b shows several nDMA oscillation curves measured on the sapphire and epoxy matrix and at two different temperatures. Clearly, the increasing temperature from 298 to 403 K did not affect the oscillation behavior of the probe in contact with the sapphire substrate. The phase shift measured on the sapphire only slightly varied by ± 2° with temperature. In contrast, there was a significant change of the phase shift values for the epoxy matrix when increasing the temperature from 298 to 403 K. This is because the epoxy sample with a T_g of ~365 K changes from a glassy to a rubbery state at 403 K and should, therefore, dissipate much more energy than it does at lower temperatures.

3. RESULTS AND DISCUSSION

The effect of nanosilica on the mechanical reinforcement of the epoxy resin in both glassy and rubbery states is investigated using the macroDMA method. Figure 2a,b presents the storage and loss moduli of neat epoxy and epoxy nanocomposites measured at 105 Hz as a function of temperature. The presence of nanosilica slightly increases these quantities, although a clear change in the loss tangent (tan δ) (Figure 2c), i.e., the ratio of the loss modulus to the storage modulus, is difficult to recognize. In fact, similar observations have also been reported for other epoxy/silica systems using fillers with different coupling agents.[44,45] However, this is quite different from the results reported for epoxy/MCNT and/or epoxy filled with soft fillers,[16,28] in which the enhancement of loss modulus and tan δ quantities for glassy epoxy composites was clearly observed when adding the fillers. Such an enhancement of the viscoelastic property has been attributed to the occurrence of faster viscoelastic relaxation processes at the epoxy/filler interfaces and/or the soft domains than in the

https://doi.org/10.1021/acsami.3c06123
ACS Appl. Mater. Interfaces 2023, 15, 38029−38038

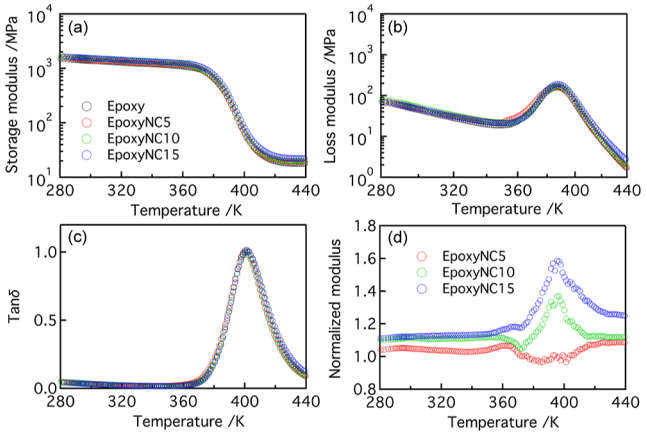

Figure 2. Temperature dependence of (a) storage modulus, (b) loss modulus, and (c) loss tangent (tan δ) measured by macroDMA at 105 Hz for neat epoxy (Epoxy) and epoxy nanocomposites with a weight fraction of 5 wt % (EpoxyNC5), 10 wt % (EpoxyNC10), and 15 wt % (EpoxyNC15). (d) Temperature dependence of the normalized modulus of different epoxy nanocomposites with respect to the neat epoxy.

matrixes, although no direct measurements at these nanoscale regions have been reported.

Figure 2d shows normalized modulus quantities as a function of temperature, which describe the magnitude of the modulus reinforcement for the epoxy nanocomposites, defined as the ratio of the sample storage modulus to that of the neat epoxy. Although the modulus enhancement can be observed in both glassy and rubbery states, it appears that the effect of nanosilica on the modulus reinforcement for rubbery epoxies is much stronger than that for glassy epoxies, which is also consistent with reported results for other epoxy/silica systems.[45] For current epoxy nanocomposites in the glassy state, we have previously revealed the existence of a soft interfacial layer surrounding nanosilica using the AM−FM AFM method,[38] which enabled us to nicely explain the reinforcement degree of the epoxy Young's modulus measured by tensile test. A detailed comparison of the modulus reinforcement for our macroDMA data measured at 298 and 403 K, that is, below and above the epoxy T_g of 365 K, respectively, with tensile results is shown in Figure S1. The macroDMA and tensile results for glassy epoxy nanocomposites are quite consistent with each other, which can be reasonably described using the Halpin−Tsai three-phase model with the incorporation of a soft interfacial layer of ∼20 nm surrounding nanosilica.[38] However, the modulus enhancement for rubbery nanocomposites is found to be much stronger than that predicted by the Halpin−Tsai model, even in the original two-phase form. This finding is indeed in good agreement with several theoretical models suggesting that the effect of temperature on the mechanical response of the interfacial polymers can be significantly different from that of the matrix.[63,64]

To confirm the presence of a soft interface surrounding nanosilica in these epoxy nanocomposites, we first use the PeakForce QNM method for a fast mapping of the elastic response at high spatial resolution, i.e., it takes about 8 min to obtain a 256 × 256 pixel image, together with recorded force-deformation cures at each pixel. Figure 3a,b shows topographic and elastic modulus maps measured by the QNM method for epoxy filled with 5 wt % nanosilica (EpoxyNC5), where the elastic map was generated by fitting the detected force-deformation curves with the JKR-based linearized method.[61,62] Nanometer-sized interfacial layers formed surrounding nanosilica can be observed in the elastic map, for which the elastic modulus is estimated to be 2−3 times smaller than the matrix

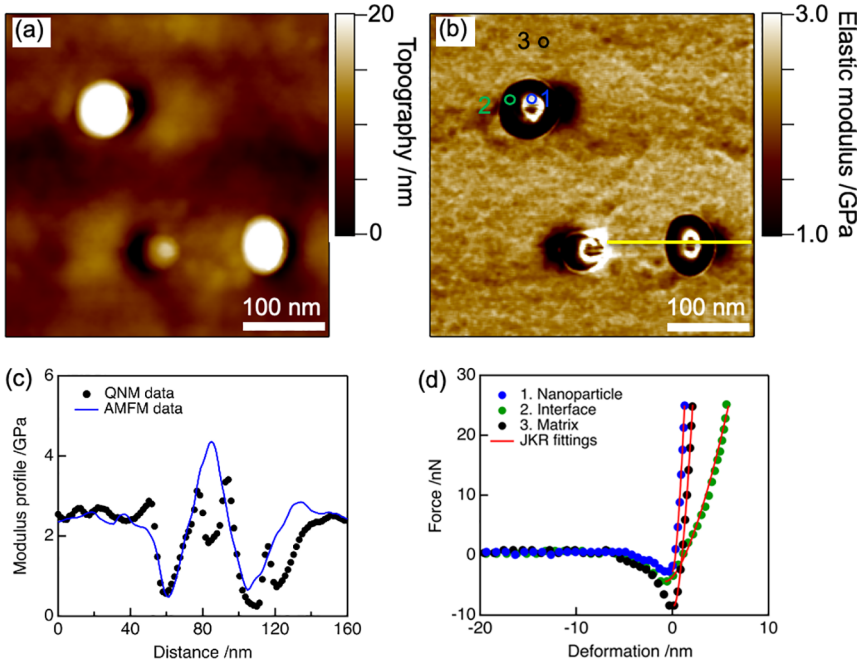

Figure 3. (a) Topographic and (b) elastic modulus images measured by the QNM method for the EpoxyNC5 sample. (c) Comparison of the modulus profiles across a nanosilica measured by QNM and AM−FM methods: the QNM data corresponds to the yellow line marked in (b), whereas the AM−FM data is imported from our previous report.[38] (d) Force−deformation curves obtained at the nanosilica, interface, and matrix regions as marked by circles in (b): red solid lines represent JKR fitting results for each experimental curve.

https://doi.org/10.1021/acsami.3c06123
ACS Appl. Mater. Interfaces 2023, 15, 38029−38038

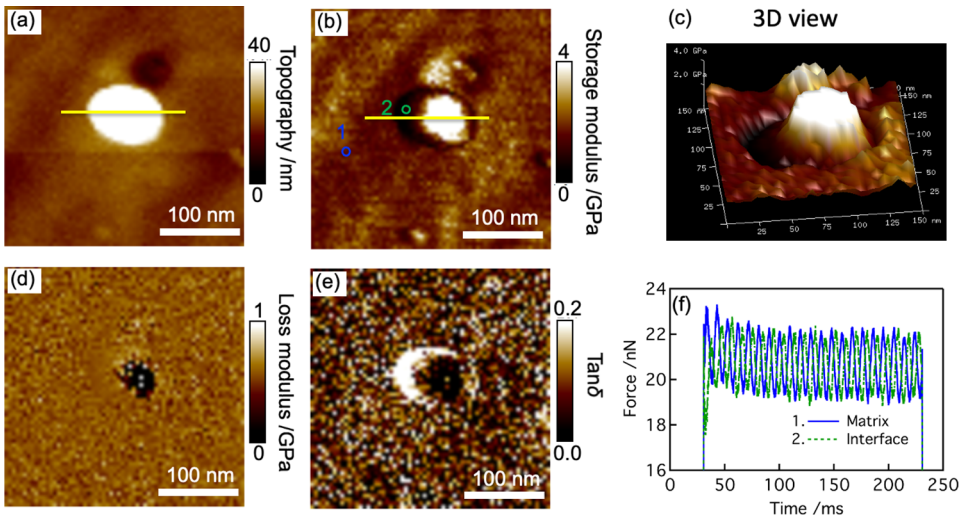

Figure 4. Several nDMA images for the EpoxyNC5 sample measured at 298 K: (a) topography, (b) storage modulus, (c) storage modulus in 3D-view, (d) loss modulus, and (e) tan δ. (f) Typical force oscillation curves extracted from the nDMA mapping dataset at the matrix and interface regions, as marked in the storage modulus image.

value. Figure 3c shows the modulus profile across the nanoparticle as indicated by yellow line in Figure 3b, which is also compared with the corresponding modulus profile measured by the AM−FM method from our previous work.[38] We could see excellent agreement between the two methods, showing a change in the elastic response of the epoxy network upon approaching the nanoparticle interface. Since the probes used in our AFM methods exhibit a calibrated radius of ∼10 nm, relatively smaller than the characteristic sizes of both the interface (∼20 nm) and nanosilica (∼50 nm), we can reasonably neglect the effect of the convolution between these nanoscale objects. In fact, by using a probe with a radius of ∼30 nm we were not able to detect the presence of an interfacial layer surrounding nanosilica, while the size of the nanosilica was almost unchanged.[38] Figure 3d compares several force-deformation curves from the nanosilica, interface, and matrix regions marked in the elastic modulus map. These curves show a clear difference in both the slope and maximum adhesive force, indicating a change in the elastic and adhesive properties of polymers crossing the nanoparticle interface. A smaller maximum adhesive force at the interface than in the matrix is consistent with the fact that the adhesive response of the interface is weaker than that of the matrix, as discussed elsewhere.[38]

Although AM−FM and QNM methods reveal the presence of a soft epoxy interface surrounding the nanosilica at high spatial resolution, neither is suitable for discussing the viscoelastic behavior of this interface, especially at rheologically relevant frequencies. We therefore employ nDMA to detail the dynamic mechanical behavior of this soft interface at multiple temperatures, from below to above the T_g. Figure 4 presents nDMA measurements over a small area of 300 × 300 nm for the EpoxyNC5 sample at 298 K. The topographic image shown in Figure 4a evidences the presence of nanosilica with a size of less than 100 nm. Figure 4b represents the nDMA storage modulus map, which provides an average modulus value of ∼2 GPa for the epoxy matrix, in good agreement with the QNM data shown in Figure 2b. A soft interface surrounding the nanosilica is visible in both 2D (Figure 4b) and 3D (Figure 4c) views, which is perfectly consistent with QNM and AM−FM results, as discussed above, although the symmetric behavior of the soft interface, as observed in the QNM and AM−FM modulus images, appears to be distorted in the nDMA modulus image. This difference might be related to the longer capturing time and lower resolution of the nDMA images, and thus the effect of the thermal drift is more severe. It is noteworthy to mention that although AM−FM and QNM/nDMA methods assume different contact mechanics models for describing the probe/sample interaction, i.e., the Hertzian model in the AM−FM and JKR model in QNM and nDMA, such an agreement between these methods for measuring the elastic modulus of glassy polymers is expected due to the dominant contribution of the elastic interaction with respect to the adhesive interaction.[49,50] Another concern is related to the state of the nanosilica at the surface under the AFM measurement, which can be different in the matrix state. Currently, it remains difficult to provide a direct effect of the filler state on the interfacial properties measured by our AFM methods because, to the best of our knowledge, there is still a lack of quantitative measurement of the local mechanical properties of nanoscale interfaces surrounding fillers in the matrix state. However, many studies have provided good agreement between AFM-based methods and conventional macroscopic techniques for quantifying the mechanical properties of polymers.[44,50,55,58] We can therefore suppose that the mechanical properties of the interfacial layer surrounding nanosilica particles at the surface measured by our AFM methods are also applicable to those dispersed within the epoxy matrix.

Figure 4d,e shows the corresponding loss modulus and tan δ images, respectively, for the captured area. Although it is difficult to distinguish the interface and matrix regions in the loss modulus image (Figure 4d), Figure 4e shows a clear increase in tan δ quantity at the interface compared to the matrix value. Since the tan δ magnitude provides a direct comparison in the viscoelastic dynamics between the matrix and interface, we can reasonably claim that the viscoelastic relaxation of polymers at the epoxy interface is stronger than that in the glassy matrix. Figure 4f provides force oscillation curves extracted from the nDMA mapping dataset at the matrix and interface regions. There is a significant deviation of the phase shift at the interface in comparison with that from the

https://doi.org/10.1021/acsami.3c06123
ACS Appl. Mater. Interfaces 2023, 15, 38029−38038

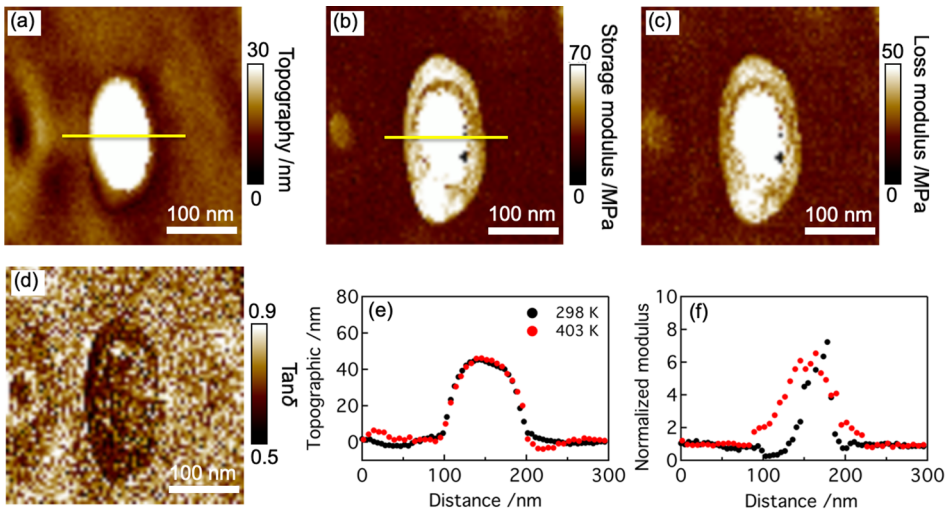

Figure 5. (a) Topography, (b) storage modulus, (c) loss modulus, and (d) tan δ images for the EpoxyNC5 sample measured at 403 K. A comparison of the (e) topographic and (f) storage modulus profiles normalized to the matrix values across the nanosilica measured at 298 and 403 K: the data correspond to the yellow lines marked in Figure 4a,b at 298 K and (a,b) at 403 K.

matrix, indicating a stronger dissipation of mechanical energy at the interface under mechanical oscillation.

Notably, the formation of the soft interface surrounding the nanosilica with enhanced viscoelasticity, as revealed by nDMA mappings, nicely resembles the epoxy composites with soft fillers, for which the toughening effects can be attributed to the viscoelastic energy dissipation.[14−16] The key difference between two systems is that the soft interfacial layer in epoxy/silica nanocomposites is well localized around nanoparticles without forming a continuous soft network, even for systems with a higher silica fraction up to 15−20 wt %, provided that the nanoparticles are well dispersed within the matrix.[29,38] Such a difference seems to be critical for controlling the modulus reinforcement of epoxy nanocomposites when using rigid nanofillers.[29,38] It is also noteworthy that the increased viscoelasticity of local polymers at the interface observed here for glassy epoxy nanocomposites nicely supports the energy dissipation mechanism via viscoelastic relaxation of nanoscale interfaces as proposed for various hard nanostructured materials,[39,42,43] which is indeed difficult to detect using the conventional macroDMA method. In addition, the enhanced energy dissipation due to the viscoelastic relaxation at the epoxy/silica interface can provide a relevant explanation for the local strain constraints observed in interfacial regions without nanovoids, as recently reported by Wang and co-workers.[41]

To extend our understanding of the mechanical relaxation at the interface, nDMA measurements were also carried out at multiple temperatures up to 423 K, that is, from a glassy to a rubbery state. Figure 5 shows representative examples of nDMA mappings for the EpoxyNC5 sample at 403 K. Data obtained at several other temperatures are provided in Figure S3. Although the shape of nanofillers becomes elongated due to the increased thermal drift when measured at elevated temperatures, the presence of an interface surrounding the nanoparticle with different mechanical properties from the matrix can still be observed in these images. As expected, the dynamic storage modulus (Figure 5b) for the epoxy matrix is drastically decreased to ∼30 MPa at 403 K. Interestingly, the storage modulus image reveals a stiffening of the interface compared to the matrix. This behavior is also found for the loss modulus quantity presented in Figure 5c, whereas the tan δ image (Figure 5d) shows a slight decrease at the interface compared to the matrix. Such a change demonstrates the complex nature of the mechanical response of the epoxy/silica interface. In fact, we also conducted nDMA mappings for the EpoxyNC15 sample at 298 and 403 K, which are provided in Figure S4. These mappings evidence the same behavior of the interface modulus, i.e., changing from softening in the glassy state to stiffening in the rubbery state with respect to the matrix modulus, for fillers of different sizes. We can therefore claim that the presence of the interfacial layer surrounding nanosilica with dynamic mechanical properties different from the matrix is common for this epoxy/silica system, independent of the fraction and size of nanosilica. These results also confirm the reproducibility of our nDMA measurement.

Figure 5e,f compares the height and storage modulus profiles across the nanoparticle obtained at 298 and 403 K, respectively. Although the height profiles are nearly independent of the temperature, the modulus profiles clearly evidence a reversed change of the interface stiffness with respect to the matrix behavior under the transition from a glassy to a rubbery state. For example, at a distance point of ∼100 nm in Figure 5e,f, while the height values are similar (∼5.0 nm above the surface), the normalized modulus values of the interface are ∼0.5 and 2.0 for the glassy and rubbery states, respectively. Similar results are also found for other nanoparticles in the EpoxyNC15 sample shown in Figure S4. One example is presented in Figure S4f, in which the height and storage modulus profiles across a smaller nanosilica are compared at 298 and 403 K, respectively. At a distance point of ∼65 nm, the normalized modulus value of the interface changes from ∼0.7 in the glassy state to ∼1.9 in the rubbery state, while the height values are ∼12 nm above the surface. Relying on this analysis, we can therefore ignore the effect of the morphology of the nanosilica on the measured modulus profile. In other words, this change is largely related to the intrinsic dependence of the mechanical property of the interface on the temperature, which can be different from that of the matrix modulus. More interestingly, the softening and stiffening behaviors of the interface in the glassy and rubbery states, respectively, nicely

https://doi.org/10.1021/acsami.3c06123
ACS Appl. Mater. Interfaces 2023, 15, 38029−38038

reflect the increase in the modulus reinforcement of these epoxy nanocomposites with increased temperature, as shown in Figure 2d.

The softening of the glassy epoxy interface can be attributed to a decreased crosslinking density of epoxy networks near the nanosilica interface.[34−37] At first glance, this change in the network structure seems not to provide a relevant explanation for the stiffening of the rubbery interface. However, as evidenced in various polymer nanocomposite systems,[63−65] not only the network structure but also the polymer dynamics can be altered upon approaching a solid interface. While the former is expected to be less dependent on temperature, the dynamics of interfacial polymers have been detected to be much slower than those of bulk polymers in a rubbery state due to the constraint effect.[63−66] Therefore, to reasonably explain our macroDMA and nDMA results for the modulus reinforcement of glassy and rubbery epoxies, we can suppose that in the glassy state, the effect originating from the difference in the crosslinking density between the interfacial and matrix regions is dominated,[37] causing the softening at the interface. In contrast, in the rubbery state the dynamic nature of polymers becomes dominant in determining the mechanical responses of the interfacial region compared to the matrix behavior.[63] The dynamics of interfacial polymers can be much slower than that of matrix polymers, thus giving rise to the enhancement of the elastic modulus at the interfaces, as generally observed in rubber nanocomposites.[48,67]

Figure 6 shows a detailed comparison of the storage modulus and tan δ quantities measured by both nDMA and macroDMA methods at a similar frequency over a broad temperature range. MacroDMA data were obtained for the neat Epoxy sample, whereas nDMA data were measured at the interfacial and matrix regions of the EpoxyNC5 sample. nDMA storage modulus and tan δ values for the matrix at each temperature are calculated by Gaussian fitting the histogram of the corresponding image, whereas these quantities for the interface are averaged over tens of pixel points around the center of the interfacial layer. The glassy matrix and interface exhibit average nDMA storage moduli of 2.1 ± 0.2 and 0.45 ± 0.05 GPa, respectively, when measured at 298 K. QNM elastic modulus values for the matrix and interface at 298 K are also presented in Figure 6a, which agree well with the corresponding data obtained by the nDMA method. The nDMA storage moduli for both the matrix and interface are unchanged when increasing temperature close to the epoxy T_g of 365 K, followed by a sudden decrease to 20−30 MPa above the T_g. This behavior is nicely consistent with the temperature dependence of the macroDMA storage modulus measured for the neat Epoxy sample, as also provided in Figure 6a. A deviation between the nanoscale data measured by AFM methods for the matrix region and the macroscopic modulus can be observed, especially in the glassy regime, which indeed has been previously reported for various polymer systems.[68−70] Such a deviation might originate from several factors, such as differences in sample geometry and the model used for calculating the modulus between AFM and macroDMA methods.

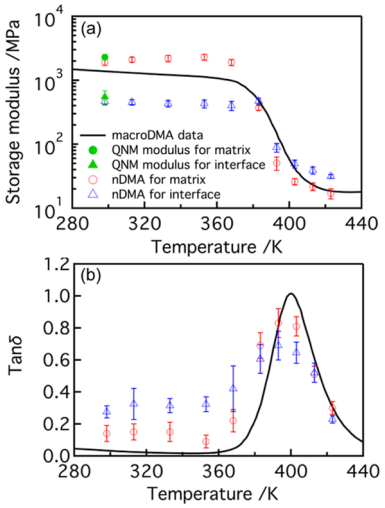

Figure 6. (a) Storage modulus and (b) tan δ data measured by nDMA and macroDMA methods at multiple temperatures. Black lines were measured by macroDMA at 105 Hz for the neat Epoxy sample. The red circle and triangle symbols were measured by nDMA at 105 Hz at the matrix and interfacial regions of the EpoxyNC5 sample, respectively. The blue circle and triangle symbols were measured by QNM at 1 kHz for the matrix and interfacial regions of the EpoxyNC5 sample, respectively.

Figure 6b shows the average nDMA tan δ values as a function of temperature for both the matrix and interface in comparison with macroDMA data. Although there exists a deviation in the magnitude between nDMA and macroDMA tan δ for the epoxy matrix, which might originate from the same reasons as the deviation of the storage modulus, the temperature dependence of this quantity shows a good agreement between the two methods. Such an agreement observed for both storage modulus and tan δ quantities strongly confirms the reliability of the new nDMA approach for quantifying dynamic mechanical properties of polymers at the nanoscale over a broad temperature range, which was previously also observed for other polymer systems.[58] Although our study here focuses on the epoxy/nanosilica system, it is expected that similar nDMA measurements are applicable for other polymer nanocomposites as long as the sizes of the nanofiller and interfacial layer are comparable or relatively larger than those of the probe radius to minimize a convolution effect, as discussed above.

Another important finding here is that the nDMA tan δ at the interface demonstrates an enhancement of this quantity at all temperatures below the sample T_g, evidencing the increased viscoelasticity of interfacial polymers compared that of the glassy epoxy matrix. This implies that the viscoelastic energy dissipation at the nanoscale interface can contribute to the toughening effects of glassy epoxy nanocomposites over a broad temperature range prior to approaching the T_g. Another interesting result is that the dependence of the storage modulus and tan δ quantities on the temperature, especially near the glass transition regime, between the interface and the epoxy matrix is quite different. For example, the decrease of the storage modulus for the matrix measured by nDMA and macroDMA occurs at around 370 K, well below that at around 380 K for the interface measured by nDMA. Also, the magnitudes of the changes in the storage modulus and tan δ quantities at the glass transition are much weaker for the interface compared to the matrix. Such a deviation in the glass transition behavior between the interface and the matrix might directly confirm a significant difference in the temperature dependence of the segmental dynamics for the interfacial and matrix polymers, as predicted in several theoretical models.[63−65]

https://doi.org/10.1021/acsami.3c06123
ACS Appl. Mater. Interfaces 2023, 15, 38029−38038

4. CONCLUSIONS

A new AFM-based nDMA approach with the probe-driving system is employed to quantify the dynamic mechanical properties of nanoscale interfaces in a model epoxy/silica nanocomposite over a broad range of temperature. Using nDMA enables us to simultaneously measure several rheological quantities, including storage and loss moduli and tan δ of polymers as a function of temperature in the same manner as a standard DMA technique. Thanks to the sharp AFM probe, we are able to obtain direct mappings of the dynamic mechanical relaxation of the nanoscale interfacial layer formed in the epoxy nanocomposite. In its glassy state, the nDMA storage modulus of the interface is found to be smaller than that of the bulk matrix, which agrees well with the results obtained by other AFM methods. By increasing the temperature from below to above the T_g, we observe a change from the softening to the stiffening of the interface modulus with respect to the matrix, which might be related to an increased deviation in the polymer dynamics between the interfacial and matrix regions upon approaching the T_g. Importantly, the nDMA tan δ image demonstrates enhanced viscoelastic relaxation at the interface with respect to the matrix at different temperatures in the glassy state. This evidence could provide important insights into better understanding the toughening effects associated with the viscoelastic energy dissipation at the interface in glassy epoxy nanocomposites. Our nDMA results also show good agreement with those measured by other well-accepted AFM methods at the nanoscale as well as macroDMA over a broad temperature range, which might initiate a new paradigm for characterizing nanoscale dynamic mechanical responses for various structural nanocomposites.

ASSOCIATED CONTENT

Supporting Information

The Supporting Information is available free of charge at https://pubs.acs.org/doi/10.1021/acsami.3c06123.

nDMA theoretical description; modulus reinforcement plots; force-deformation curves; and nDMA images (PDF).

AUTHOR INFORMATION

Corresponding Authors

Keiji Tanaka − *Center for Polymer Interface and Molecular Adhesion Science, Kyushu University, Fukuoka 819-0395, Japan; Department of Applied Chemistry, Kyushu University, Fukuoka 819-0395, Japan;* orcid.org/0000-0003-0314-3843; Email: k-tanaka@cstf.kyushu-u.ac.jp

Ken Nakajima − *Department of Chemical Science and Engineering, School of Materials and Chemical Technology, Tokyo Institute of Technology, Tokyo 152-8552, Japan;* orcid.org/0000-0001-7495-0445; Email: nakajima.k.aa@m.titech.ac.jp

Authors

Hung K. Nguyen − *Department of Chemical Science and Engineering, School of Materials and Chemical Technology, Tokyo Institute of Technology, Tokyo 152-8552, Japan;* orcid.org/0000-0002-5398-2533

Atsuomi Shundo − *Center for Polymer Interface and Molecular Adhesion Science, Kyushu University, Fukuoka 819-0395, Japan;* orcid.org/0000-0002-7898-3233

Makiko Ito − *Department of Chemical Science and Engineering, School of Materials and Chemical Technology, Tokyo Institute of Technology, Tokyo 152-8552, Japan*

Bede Pittenger − *Bruker Nano Surfaces, Santa Barbara, California 93117, United States;* orcid.org/0000-0002-5980-878X

Satoru Yamamoto − *Center for Polymer Interface and Molecular Adhesion Science, Kyushu University, Fukuoka 819-0395, Japan;* orcid.org/0000-0002-0238-3039

Complete contact information is available at: https://pubs.acs.org/10.1021/acsami.3c06123

Notes

The authors declare no competing financial interest.

ACKNOWLEDGMENTS

We thank Dr. M. Aoki for preparing the samples and for fruitful discussions of the results. This work was supported by the JST-Mirai Program Grant Number JPMJMI18A2, Japan.

REFERENCES

(1) Garces, J. M.; Moll, D. J.; Bicerano, J.; Fibiger, R.; McLeod, D. G. Polymeric Nanocomposites for Automotive Applications. *Adv. Mater.* **2000**, *12*, 1835−1839.

(2) Njuguna, J.; Pielichowski, K. Polymer Nanocomposites for Aerospace Applications: Properties. *Adv. Eng. Mater.* **2003**, *5*, 769−778.

(3) Balazs, A. C.; Emrick, T.; Russell, T. P. Nanoparticle Polymer Composites: Where two Small Worlds Meet. *Science* **2006**, *314*, 1107−1110.

(4) Naskar, A. K.; Keum, J. K.; Boeman, R. G. Polymer Matrix Nanocomposites for Automotive Structural Components. *Nat. Technol.* **2016**, *11*, 1026−1030.

(5) Higgins, A. Adhesive Bonding of Aircraft Structures. *Int. J. Adhes. Adhes.* **2000**, *20*, 367−376.

(6) Jin, F. L.; Li, X.; Park, S. J. Synthesis and Application of Epoxy Resins: A Review. *J. Ind. Eng. Chem.* **2015**, *29*, 1−11.

(7) Gu, H.; Ma, C.; Gu, J.; Guo, J.; Yan, X.; Huang, J.; Zhang, Q.; Guo, Z. An Overview of Multifunctional Epoxy Nanocomposites. *J. Mater. Chem. C* **2016**, *4*, 5890−5906.

(8) Shundo, A.; Yamamoto, S.; Tanaka, K. Network Formation and Physical Properties of Epoxy Resins for Future Practical Applications. *JACS Au* **2022**, *2*, 1522−1542.

(9) Guild, F. J.; Tsang, W. L.; Taylor, A. C. Silica Nano-Particle Filled Polymers: Debonding and Microstructure. *Compos. Sci. Technol.* **2022**, *218*, 109202.

(10) Kinloch, A. J. Toughening Epoxy Adhesives to Meet Today's Challenges. *Mater. Res. Soc. Bull.* **2003**, *28*, 445−448.

(11) Wetzel, B.; Rosso, P.; Haupert, F.; Friedrich, K. Epoxy Nanocomposites − Fracture and Toughening Mechanisms. *Eng. Fract. Mech.* **2006**, *73*, 2375−2398.

(12) Van Velthem, P.; Ballout, W.; Horion, J.; Janssens, Y.-A.; Destoop, V.; Pardoen, T.; Bailly, C. Morphology and Fracture Properties of Toughened Highly Crosslinked Epoxy Composites: A Comparative Study between High and Low T_g Tougheners. *Composites, Part B* **2016**, *101*, 14−20.

(13) Quaresimin, M.; Schulte, K.; Zappalorto, M.; Chandrasekaran, S. Toughening Mechanisms in Polymer Nanocomposites: from Experiments to Modeling. *Compos. Sci. Technol.* **2016**, *123*, 187−204.

(14) Liu, J. D.; Thompson, Z. J.; Sue, H.-J.; Bates, F. S.; Hillmyer, M. A.; Dettloff, M.; Jacob, G.; Verghese, N.; Pham, H. Toughening of Epoxies with Block Copolymer Micelles of Wormlike Morphology. *Macromolecules* **2010**, *43*, 7238−7243.

(15) Pruksawan, S.; Samitsu, S.; Yokoyama, H.; Naito, M. Homogeneously Dispersed Polyrotaxane in Epoxy Adhesive and Its

Improvement in Fracture Toughness. *Macromolecules* **2019**, *52*, 2464−2475.
(16) Hanafusa, A.; Ando, S.; Ozawa, S.; Ito, M.; Hasegawa, R.; Mayumi, K.; Ito, K. Viscoelastic Relaxation Attributed to the Molecular Dynamics of Polyrotaxane Confined in an Epoxy Network. *Polym. J.* **2020**, *52*, 1211−1221.
(17) Kinloch, A. J.; Mohammed, R. D.; Taylor, A. C.; Eger, C.; Sprenger, S.; Egan, D. The Effect of Silica Nano Particles and Rubber Particles on the Toughness of Multiphase Thermosetting Epoxy Polymers. *J. Mater. Sci.* **2005**, *40*, 5083−5086.
(18) Hsieh, T. H.; Kinloch, A. J.; Masania, K.; Sohn Lee, J.; Taylor, A. C.; Sprenger, S. The Toughness of Epoxy Polymers and Fibre Composites Modified with Rubber Microparticles and Silica Nanoparticles. *J. Mater. Sci.* **2010**, *45*, 1193−1210.
(19) Liu, H.-Y.; Wang, G.-T.; Mai, Y.-W.; Zeng, Y. On Fracture Toughness of Nano-particle Modified Epoxy. *Composites, Part B* **2011**, *42*, 2170−2175.
(20) Zappalorto, M.; Pontefisso, A.; Fabrizi, A.; Quaresimin, M. Mechanical Behaviour of Epoxy/Silica Nanocomposites: Experiments and Modeling. *Composites, Part A* **2015**, *72*, 58−64.
(21) Picu, C. R.; Krawczyk, K. K.; Wang, Z.; Pishvazadeh-Moghaddam, H.; Sieberer, M.; Lassnig, A.; Kern, W.; Hadar, A.; Constantinescu, D. M. Toughening in Nanosilica-Reinforced Epoxy with Tunable Filler-Matrix Interface Properties. *Compos. Sci. Technol.* **2019**, *183*, 107799.
(22) Zhao, S.; Schadler, L. S.; Duncan, R.; Hillborg, H.; Auletta, T. Mechanisms Leading to Improved Mechanical Performance in Nanoscale Alumina Filled Epoxy. *Compos. Sci. Technol.* **2008**, *68*, 2965−2975.
(23) Rafiee, M. A.; Rafiee, J.; Wang, Z.; Song, H.; Yu, Z.-Z.; Koratkar, N. Enhanced Mechanical Properties of Nanocomposites at Low Graphene Content. *ACS Nano* **2009**, *3*, 3884−3890.
(24) Tang, L.-C.; Wan, Y.-J.; Peng, K.; Pei, Y.-B.; Wu, L.-B.; Chen, L.-M.; Shu, L.-J.; Jiang, J.-X.; Lai, G.-Q. Fracture Toughness and Electrical Conductivity of Epoxy Composites Filled with Carbon Nanotubes and Spherical Particles. *Composites, Part A* **2013**, *45*, 95−101.
(25) Domun, N.; Hadavinia, H.; Zhang, T.; Sainsbury, T.; Liaghat, G. H.; Vahid, S. Improving the Fracture Toughness and the Strength of Epoxy Using Nanomaterials − a Review of the Current Status. *Nanoscale* **2015**, *7*, 10294−10329.
(26) Pruksawan, S.; Samitsu, S.; Fujii, Y.; Torikai, N.; Naito, M. Toughening Effect of Rodlike Cellulose Nanocrystals in Epoxy Adhesive. *ACS Appl. Polym. Mater.* **2020**, *2*, 1234−1243.
(27) Chi, H.; Zhang, G.; Wang, N.; Wang, Y.; Li, T.; Wang, F.; Ye, C. Enhancing the Mechanical Strength and Toughness of Epoxy Resins with Linear POSS Nano-modifier. *Nanoscale Adv.* **2022**, *4*, 1151−1157.
(28) Suhr, J.; Koratkar, N.; Keblinski, P.; Ajayan, P. Viscoelasticity in Carbon Nanotube Composites. *Nat. Mater.* **2005**, *4*, 134−137.
(29) Johnsen, B. B.; Kinloch, A. J.; Mohammed, R. D.; Taylor, A. C.; Sprenger, S. Toughening Mechanisms of Nanoparticle-Modified Epoxy Polymers. *Polymer* **2007**, *48*, 530−541.
(30) Zappalorto, M.; Salviato, M.; Quaresimin, M. Influence of the Interphase Zone on the Nanoparticle Debonding Stress. *Compos. Sci. Technol.* **2011**, *72*, 49−55.
(31) Hua, Y.; Gu, L.; Premaraj, S.; Zhang, X. Role of Interphase in the Mechanical Behavior of Silica/Epoxy Resin Nanocomposites. *Materials* **2015**, *8*, 3519−3531.
(32) Xu, W.; Ma, H.; Ji, S.; Chen, H. Analytical Effective Elastic Properties of Particulate Composites with Soft Interfaces around Anisotropic Particles. *Compos. Sci. Technol.* **2016**, *129*, 10−18.
(33) Kim, B.; Choi, J.; Yang, S.; Yu, S.; Cho, M. Multiscale Modeling of Interphase in Crosslinked Epoxy Nanocomposites. *Composites, Part B* **2017**, *120*, 128−142.
(34) Putz, K. W.; Palmeri, M. J.; Cohn, R. B.; Andrews, R.; Brinson, L. C. Effect of Cross-Link Density on Interphase Creation in Polymer Nanocomposites. *Macromolecules* **2008**, *41*, 6752−6756.
(35) Yamamoto, S.; Kuwahara, R.; Aoki, M.; Shundo, A.; Tanaka, K. Molecular Events for an Epoxy-Amine System at a Copper Interface. *ACS Appl. Polym. Mater.* **2020**, *2*, 1474−1481.
(36) Ghasem Zadeh Khorasani, M.; Silbernagl, D.; Szymoniak, P.; Hodoroaba, V.-D.; Sturm, H. The Effect of Boehmite Nanoparticles (γ-AlOOH) on Nanomechanical and Thermomechanical Properties Correlated to Crosslinking Density of Epoxy. *Polymer* **2019**, *164*, 174−182.
(37) Sirovica, S.; Solheim, J. H.; Skoda, M. W. A.; Hirschmugl, C. J.; Mattson, E. C.; Aboualizadeh, E.; Guo, Y.; Chen, X.; Kohler, A.; Romanyk, D. L.; Rosendahl, S. M.; Morsch, S.; Martin, R. A.; Addison, O. Origin of Micro-Scale Heterogeneity in Polymerization of Photo-Activated Resin Composites. *Nat. Commun.* **2020**, *11*, 1849.
(38) Nguyen, H. K.; Shundo, A.; Liang, X.; Yamamoto, S.; Tanaka, K.; Nakajima, K. Unraveling Nanoscale Elastic and Adhesive Properties at the Nanoparticle/Epoxy Interface Using Bimodal Atomic Force Microscopy. *ACS Appl. Mater. Interfaces* **2022**, *14*, 42713−42722.
(39) Smith, B. L.; Schaffer, T. E.; Viani, M.; Thompson, J. B.; Frederick, N. A.; Kindt, J.; Belcher, A.; Stucky, G. D.; Morse, D. E.; Hansma, P. K. Molecular Mechanistic Origin of the Toughness of Natural Adhesives, Fibres and Composites. *Nature* **1999**, *399*, 761−763.
(40) Burghard, Z.; Zini, L.; Srot, V.; Bellina, P.; Aken, P. A. v.; Bill, J. Toughening through Nature-Adapted Nanoscale Design. *Nano Lett.* **2009**, *9*, 4103−4108.
(41) Wang, P.; Maeda, R.; Aoki, M.; Kubozono, T.; Yoshihara, D.; Shundo, A.; Kobayashi, T.; Yamamoto, S.; Tanaka, K.; Yamada, S. In Situ Transmission Electron Microscopy Observation of the Deformation and Fracture Processes of an Epoxy/Silica Nanocomposite. *Soft Matter* **2022**, *18*, 1149−1153.
(42) Wegst, U. G. K.; Bai, H.; Saiz, E.; Tomsia, A. P.; Ritchie, R. O. Bioinspired Structural Materials. *Nat. Mater.* **2015**, *14*, 23−36.
(43) Barthelat, F.; Yin, Z.; Buehler, M. J. Structure and Mechanics of Interfaces in Biological Materials. *Nat. Rev. Mater.* **2016**, *1*, 16007.
(44) Wetzel, B.; Haupert, F.; Qiu Zhang, M. Epoxy Nanocomposites with High Mechanical and Tribological Performance. *Compos. Sci. Technol.* **2003**, *63*, 2055−2067.
(45) Guo, Q.; Zhu, P.; Li, G.; Wen, J.; Wang, T.; Lu, D. D.; Sun, R.; Wong, C. Study on the Effects of Interfacial Interaction on the Rheological and Thermal Performance of Silica Nanoparticles Reinforced Epoxy Nanocomposites. *Composites, Part B* **2017**, *116*, 388−397.
(46) Chyasnavichyus, M.; Young, S. L.; Tsukruk, V. V. Probing of Polymer Surfaces in Viscoelastic Regime. *Langmuir* **2014**, *30*, 10566−10582.
(47) Kocun, M.; Labuda, A.; Meinhold, W.; Revenko, I.; Proksch, R. Fast, High Resolution, and Wide Modulus Range Nanomechanical Mapping with Bimodal Tapping Mode. *ACS Nano* **2017**, *11*, 10097−10105.
(48) Wang, D.; Russell, T. P. Advances in Atomic Force Microscopy for Probing Polymer Structure and Properties. *Macromolecules* **2018**, *51*, 3−24.
(49) Garcia, R. Nanomechanical Mapping of Soft Materials with the Atomic Force Microscope: Methods, Theory and Applications. *Chem. Soc. Rev.* **2020**, *49*, 5850−5884.
(50) Collinson, D. W.; Sheridan, R. J.; Palmeri, M. J.; Brinson, L. C. Best Practices and Recommendations for Accurate Nanomechanical Characterization of Heterogeneous Polymer Systems with Atomic Force Microscopy. *Prog. Polym. Sci.* **2021**, *119*, 101420.
(51) Gisbert, V. G.; Benaglia, S.; Uhlig, M. R.; Proksch, R.; Garcia, R. High-Speed Nanomechanical Mapping of the Early Stages of Collagen Growth by Bimodal Force Microscopy. *ACS Nano* **2021**, *15*, 1850−1857.
(52) Dokukin, M.; Sokolov, I. High-Resolution High-Speed Dynamic Mechanical Spectroscopy of Cells and Other Soft Materials with the Help of Atomic Force Microscopy. *Sci. Rep.* **2015**, *5*, 12630.
(53) Kolluru, P. V.; Eaton, M. D.; Collinson, D. W.; Cheng, X.; Delgado, D. E.; Shull, K. R.; Brinson, L. C. AFM-based Dynamic

https://doi.org/10.1021/acsami.3c06123
ACS Appl. Mater. Interfaces 2023, 15, 38029−38038

Scanning Indentation (DSI) Method for Fast, High-Resolution Spatial Mapping of Local Viscoelastic Properties in Soft Materials. *Macromolecules* **2018**, *51*, 8964−8978.
(54) Killgore, J. P.; DelRio, F. W. Contact Resonance Force Microscopy for Viscoelastic Property Measurements: from Fundamentals to State-of-the-Art Applications. *Macromolecules* **2018**, *51*, 6977−6996.
(55) Ueda, E.; Liang, X.; Ito, M.; Nakajima, K. Dynamic Moduli Mapping of Silica-Filled Styrene-Butadiene Rubber Vulcanizate by Nanorheological Atomic Force Microscopy. *Macromolecules* **2019**, *52*, 311−319.
(56) Lefevre, M.; Tran, T. Q.; De Muijlder, T.; Pittenger, B.; Flammang, P.; Hennebert, E.; Leclere, P. On the Nanomechanical and Viscoelastic Properties of Coatings Made of Recombinant Sea Star Adhesive Proteins. *Front. Mech. Eng.* **2021**, *7*, 667491.
(57) Arai, M.; Ueda, E.; Liang, X.; Ito, M.; Kang, S.; Nakajima, K. Viscoelastic Maps Obtained by Nanorheological Atomic Force Microscopy with Two Different Driving Systems. *Jpn. J. Appl. Phys.* **2018**, *57*, 08NB08.
(58) Pittenger, B.; Osechinskiy, S.; Yablon, D.; Mueller, T. Nanoscale DMA with the Atomic Force Microscope: a New Method for Measuring Viscoelastic Properties of Nanostructured Polymer Materials. *JOM* **2019**, *71*, 3390−3398.
(59) Wang, D.; Zhang, J.; Ma, G.; Fang, Y.; Liu, L.; Wang, J.; Sun, T.; Zhang, C.; Meng, X.; Wang, K.; Han, Z.; Niu, S.; Ren, L. A Selective-Response Bioinspired Strain Sensor Using Viscoelastic Material as Middle Layer. *ACS Nano* **2021**, *15*, 19629−19639.
(60) Aoki, M.; Shundo, A.; Kuwahara, R.; Yamamoto, S.; Tanaka, K. Mesoscopic Heterogeneity in the Curing Process of an Epoxy-Amine System. *Macromolecules* **2019**, *52*, 2075−2082.
(61) Sun, Y.; Akhremitchev, B.; Walker, G. C. Using the Adhesive Interaction between Atomic Force Microscopy Tips and Polymer Surfaces to Measure the Elastic Modulus of Compliant Samples. *Langmuir* **2004**, *20*, 5837−5845.
(62) Fujinami, S.; Ueda, E.; Nakajima, K.; Nishi, T. Analytical Methods to Derive the Elastic Modulus of Soft and Adhesive Materials from Atomic Force Microscopy Force Measurements. *J. Polym. Sci., Part B: Polym. Phys.* **2019**, *57*, 1279−1286.
(63) Berriot, J.; Montes, H.; Lequeux, F.; Long, D.; Sotta, P. Evidence for the Shift of the Glass Transition near the Particles in Silica-Filled Elastomers. *Macromolecules* **2002**, *35*, 9756−9762.
(64) Starr, F. W.; Douglas, J. F.; Meng, D.; Kumar, S. K. Bound Layers "Cloak" Nanoparticles in Strongly Interacting Polymer Nanocomposites. *ACS Nano* **2016**, *10*, 10960−10965.
(65) Fukahori, Y. Generalized Concept of the Reinforcement of Elastomers. Part 1: Carbon Black Reinforcement of Rubbers. *Rubber Chem. Technol.* **2007**, *80*, 701−725.
(66) Nguyen, H. K.; Sugimoto, S.; Konomi, A.; Inutsuka, M.; Kawaguchi, D.; Tanaka, K. Dynamics Gradient of Polymer Chains near a Solid Interface. *ACS Macro Lett.* **2019**, *8*, 1006−1011.
(67) Tian, C.; Cui, J.; Ning, N.; Zhang, L.; Tian, M. Quantitative Characterization of Interfacial Properties of Carbon Black/Elastomer Nanocomposites and Mechanism Exploration on Their Interfacial Interaction. *Compos. Sci. Technol.* **2022**, *222*, 109367.
(68) Liu, H.; Chen, N.; Fujinami, S.; Louzguine-Luzgin, D.; Nakajima, K.; Nishi, T. Quantitative Nanomechanical Investigation on Deformation of Poly(lactic acid). *Macromolecules* **2012**, *45*, 8770−8779.
(69) Bahrami, A.; Morelle, X.; Hông Minh, L. D.; Pardoen, T.; Bailly, C.; Nysten, B. Curing Dependent Spacial Heterogeneity of Mechanical Response in Epoxy Resins Revealed by Atomic Force Microscopy. *Polymer* **2015**, *68*, 1−10.
(70) Nguyen, H. K.; Aoki, M.; Liang, X.; Yamamoto, S.; Tanaka, K.; Nakajima, K. Local Mechanical Properties of Heterogeneous Nanostructures Developed in a Cured Epoxy Network: Implications for Innovative Adhesion Technology. *ACS Appl. Nano Mater.* **2021**, *4*, 12188−12196.

https://doi.org/10.1021/acsami.3c06123
ACS Appl. Mater. Interfaces 2023, 15, 38029−38038